

Metal mobilization and zinc-rich circum-neutral mine drainage from the abandoned mining area of Osor (Girona, NE Spain).

Andrés Navarro¹ · Xavier Font² · Manuel Viladevall²

¹ Department of Fluid Mechanics, School of Industrial and Aeronautical Engineering of Terrassa (ETSEIAT), Universitat Politècnica de Catalunya, Colón 7–11, 08222 Terrassa, Spain. *E-mail address:* navarro@mf.upc.edu. ² Department of Geochemistry, Petrology and Geological Prospecting, University of Barcelona, Faculty of Geology, Zona Universitaria de Pedralbes, Barcelona (Spain).

Abstract. In the abandoned Osor mining area in Spain the uncontrolled dumping of mine wastes and the spill of mine drainage contributed, in spite of neutral pH conditions, to the metal mobilization and the subsequent contamination of surface water, groundwater and soils. Contaminated soil and mine wastes contained high amounts of Cd, Co, Pb, Zn, As, Ba, and Sb, above the regulated levels in Catalonia for soils of industrial use.

Mine water from the Coral adit which was the main dewatering system in the Osor area, generally, had neutral pH from carbonate and silicate dissolution, and showed high concentrations of Fe, Mn, Ni, Pb, and Zn. Geochemical modeling showed that a possible solid phase sink for Zn was smithsonite and, possibly, hydrozincite ($\text{Zn}_5(\text{OH})_6(\text{CO}_3)_2$) which could precipitate. Metal mobilization from the Coral adit is the main environmental concern of this area, which releases a significant quantity of Zn and SO_4^{2-} to the Osor creek, contaminating the surface waters.

Keywords Mine wastes; zinc; metals; leaching; soils; tailings; geochemical modeling; bioaccumulation

Introduction

In old mining areas, such as the abandoned mining district of Osor (Girona, NE Spain), the exploitation of F-Ba-Pb-Zn ores until 1980 generated an important source of contamination by cadmium, lead, zinc and other metals in surface waters, groundwater, and soils located in the vicinity of the main mine-waste impoundments. The main consequences of unremediated mine sites containing sulfide minerals, mainly pyrite and pyrrhotite, are the generation of acidic mine drainage waters and the possible mobilization of metals and metalloids (Plumlee et al. 1999; Lottermoser 2003).

However, many toxic metals, such as As, Co, Ni, Sb and Zn, are soluble at near-neutral pH and can potentially contaminate mine effluents, even without acidic conditions (Plante et al. 2011). Thus, depending on the neutralization capacity of the mining wastes, tailings, and ore host rocks, the production of neutral mine waters may be of environmental concern. Although less well documented, neutral mine drainage may also constitute a significant environmental problem due to the mobilization of metalloids such as As, Sb, Se, and metals such as Cd, Pb, and Zn (Heikkinen et al. 2009; Plante et al. 2011; Jang and Kwon 2011). The geochemistry of the mineral-water interaction is dependent on the ore and gangue minerals, local water chemistry, and geologic setting. Some authors have shown the relationship

between the types of mineral deposits and their environmental signature (Plumlee et al. 1999; Seal and Foley 2002; Seal and Hammarstrom 2003; Seal et al. 2008). Thus, the drainage-water compositions of polymetallic vein and related deposits that contain significant carbonate minerals in their gangue or wallrock alteration tend to have near-neutral pH, and elevated concentrations of Zn and Cu (Plumlee et al. 1999). Polymetallic replacement deposits hosted by carbonate sedimentary rocks tend to have mine-drainage water compositions with near-neutral pH and elevated concentrations of dissolved As, Fe, Sb, SO_4^{2-} and Zn may be generated under these conditions (Plumlee et al. 1999; Al et al. 2000; Navarro et al. 2004; Lee et al. 2005; Navarro and Cardellach 2009; Lindsay et al. 2009). Also, elevated concentrations of Mn, Ni, and Fe in pore water from low sulfide tailings from Ni-Cu sulfide ores was documented by Heikkinen et al. (2009) and Heikkinen and Räsänen (2009).

The neutral pH conditions of these waters may be attributed to the dissolution of acid-consuming carbonate minerals associated with carbonate gangue or host rocks. In some situations, precipitation of jarosite, gypsum, goethite, Fe oxy-hydroxides, siderite, and other secondary phases control Ca, Fe, Na, K, SO_4^{2-} and trace element concentrations (Blowes et al. 1994, 1998; Jurjovec et al. 2002; Navarro and Martínez 2010). Even when carbonate rocks host the affected aquifers, the near-neutral groundwater may show high dissolved concentrations of As, Fe, Ni, SO_4^{2-} , Zn, Cd, and Pb (Younger 2000; Blowes et al. 1998; Ezekwe et al. 2013).

The main objectives of this study were to estimate metal mobilization and release of toxic elements (especially Pb and Zn) from mine wastes and mine waters, conducting tests both in the laboratory (leaching tests) and in the field. In addition, geochemical modeling was used in order to evaluate the geochemical processes that may explain the geochemistry of mine water, surface water, and leachates.

Study area

The abandoned Osor mining area (Fig. 1) lies some 35 km SE of Girona, in the La Selva basin and Montseny-Guilleries massif, which forms part of the Catalanian Coastal Range (CCR) in the NE section of the Iberian Peninsula. The main mineral deposits are located in the Montseny-Guilleries massif and occur as stratabound and vein deposits associated with igneous and metasedimentary rocks of Paleozoic age (Fig. 1). These Paleozoic formations comprise the Lower Infra-Caradocian medium to high-grade metamorphic sequence, which can be divided into the high-grade Osor complex and the medium to low-grade Susqueda complex (Durán 1990; Reche et al. 2002) that are two pelitic series separated by orthogneiss.

Fig.1

Stratigraphically above lies the St. Martí Sacalm Caradocian volcano-sedimentary formation, the Silurian black slates and the carbonatic Devonian St. Martí de Llémana formation. The Paleozoic sequence shows a low and high-grade metamorphism (amphibolite facies) associated with the Variscan orogeny. The Paleozoic materials were intruded by post-tectonic granitoids, mainly biotite granodiorites of calc-alkaline composition (Enrique 1990).

The main deposits exploited in this area were the stratabound polymetallic deposits of Pb-Fe-Ba in the Bonmatí sector (Fig. 1), associated with Susqueda

Complex marbles and the F-Ba-Pb-Zn vein deposits of possible Jurassic age in the Osor area (Piqué et al. 2008). Thus, several mineralized veins formed at low temperatures are found enclosed within the Paleozoic (Cardellach et al. 1990; Canals and Cardellach 1997; Piqué et al. 2008). These veins include the following:

- Pb-rich veins of predominantly carbonate gangue (dolomite and ankerite) with significant vertical development that are enclosed exclusively within the Hercynian basement (south of the CCR).
- Metal-poor and fluorite-rich veins that are also enclosed within the basement (Osor veins).
- Barite-rich veins that are associated with normal faults and minor sulfides (Bonmatí sector).

The Osor vein deposit is located 4km SE of the Anglés town, and includes several geologically similar and thick (1–4 m) fluorite-barite-sphalerite-galena veins, exploited to a depth of 300 m. Gangue minerals include quartz, barite, calcite, pyrite, and silicates (mainly muscovite, albite and biotite). Exploitation of these veins concluded in 1980, after reaching yearly productions of 20000–30000 t of fluorite, 2000 t of Pb concentrates, and 3000 t of Zn concentrates. The Osor flotation tailings were homogeneous in grain size and composition, occupying an area of 3150 m² with a mean thickness of 15 m and comprised a total affected volume of 60000 m³. Mine drainage was mainly through the Coral adit (Fig. 1), which drains the Osor vein system with an estimated discharge into the Osor Creek of between 300 and 1100 m³/day of near neutral contaminated mine water. On an annual basis, mine water discharge was highest in the autumn or spring, and generally lowest in the late summer and early winter.

The area studied is characterized by a typically Mediterranean climate, with a mean yearly rainfall of 736 mm and a mean annual temperature of 15 °C, with mean maximum and minimum temperatures of 21.1 and 9.5 °C, respectively. The only important water course in the area is the Ter River and its tributary, the Osor creek, which receives contaminated sediment and episodic draining waters from the Osor tailings area, and contaminated mine water from the Coral adit. Estimated mean discharge of the Ter River varied widely throughout the year, ranging from 3-15 m³/s in the summer to 17–52 m³/s in the wet period, mainly during early spring and fall.

Materials and methods

Geochemistry and mineralogy of mineralization, mine wastes and soil

The locations of the sampling sites are marked on Fig. 1. The Osor soils (OS-6, OS-7, OS-10 and OS-11) were sampled close (<3 m) to the water samples, including a sample of contaminated sediments of the Coral adit (OS-8) and stream sediments (Sample OS-9). In the Osor mining area, flotation tailings (TOS sample in Table 2) and mining waste dumps (sample EM-1 in Table 2) located close to the main extraction area (Leonor shaft) were sampled, together with ore samples from the outcropping vein system. Tree leaves from *Populus nigra* (black poplars) were also sampled from the bank of the Osor

creek, at locations near the soil and water sampling points (O6 to O-10), retaining the same code of nearing soil and water samples. *Populus nigra* was used because their efficiency to detect pollution associated to Co, Cr, Fe, Hg Sb, Cu, Ni, Pb and Zn (Viladevall et al. 2007). Water, plant materials, soils, and wastes in the study area were characterized during four sampling campaigns conducted between 2009 and September 2010. Soil and mine wastes were collected with a plastic device and were stored and transported in hermetically sealed plastic bags.

Identification and analysis of the mineral phases in selected samples were performed in the laboratories of the University of Barcelona (UB). We used X-ray diffraction (XRD) for selected samples. Once the materials had been dried and ground, the total concentrations of Au, Ag, As, Ba, Br, Ca, Co, Cr, Cs, Fe, Hf, Hg, Ir, Mo, Na, Ni, Rb, Sb, Sc, Se, Sn, Sr, Ta, Th, U, W, Zn, La, Ce, Nd, Sm, Eu, Tb, Yb, and Lu, were determined using instrumental neutron activation analysis (INAA) in Actlabs (Ontario, Canada). In addition, the concentrations of the following elements were determined by acid digestion and subsequent analysis by inductively coupled plasma atomic emission spectrometry (ICP-AES): Ag, Cd, Cu, Mn, Mo, Ni, Pb, Zn, Al, Be, Bi, Ca, K, Mg, P, Sr, Ti, V, Y, and S. Samples of *Populus nigra* were dried below 60°C, macerated and a 15g aliquot was compressed into a briquette and analyzed using INAA at Actlabs.

The grain size distribution of mining wastes (sample EM-1) and tailings (sample TOS) was determined by sieving (RETSCH AS 200), the porosity by water displacement in a test tube, and field capacity by numerical methods.

Waters

Three surface water (OS-6, OS-7, OS-8), one spring (OS-10), and two mine water from the Coral adit (OS-8, OS-11) (Fig. 1, were collected between 2009 and 2010. Water sampling comprised four campaigns: winter 2009–2010 (OS-6 (W) to OS-10(W)), summer 2009 (OS-11(S)) and 2010 (OS-6(S) to OS-10(S)) and autumn 2010 (OS-6(A) to OS-10(A)).

The pH, redox potential (Eh), temperature and electrical conductivity (EC) measurement were calibrated using standard solutions and measured in situ with portable devices (HACH model sensION TM378). The samples were filtered using a cellulose nitrate membrane with a pore size of 0.45 µm. The samples for cation analysis were later acidified to pH<2.0 by adding ultra-pure HNO₃. The samples were collected in 110 mL high-density polypropylene bottles, sealed with a double cap, and stored in a refrigerator until analysis. Metal concentrations were measured by inductively coupled plasma mass spectrometry (ICP-MS) at the ACTLABS laboratories. Concentrations of chloride, nitrate and sulfate were analyzed on unfiltered samples which were filtered later with 0.45µm filters in the laboratory, by ion chromatography (IC). Water alkalinity was analyzed by titration with 0.01 HCl. Standard reference material NIST 1640 (ICPMS) was used to confirm accuracy. In order to preserve the carbonate equilibrium and CO₂ (g) levels in water samples, the samples were quickly closed and rapidly taken to the laboratory after sampling.

Flow-rate quantification of the Coral adit was performed, during the water sampling, using a broad-crested weir, which is a structure in an open channel

that has a horizontal crest above which the fluid pressure may be considered hydrostatic (Munson et al. 2009).

Column leaching experiments

Two column experiments were implemented to leach mining wastes and flotation tailings of the Osor sector (samples EM-1 and TOS, respectively, in Table 2). The column leaching method was a modified PrEN 14405 procedure, the standard European percolation test (SAIC, 2003).

The experiments were carried out for 360 minutes with 6 leachates were taken at the end of the column. The first leachate (TOS-1 and EM-1 in Table 5) was obtained after approximately 60 minutes of pumping. In addition, in-situ electrical conductivity, Eh and pH were measured. In the column experiments, we used a column with the following dimensions: 750 mm long, 150 mm diameter and 5 mm thick. At the bottom of the column and attached to it was a plastic funnel that was 222 mm long with an internal diameter of 186 mm. Inside this was a fiberglass plate with holes in it, which acted as a support column. Methacrylate was coated onto a mesh that acted as a filter and retained the porous medium. The leaching low mineralized water (LMW), similar to distilled water, was introduced into the column using a rain simulator connected to a metering pump. To simulate the possible effects of rainfall on the waste, the flow of water was designed so that it can be adjusted from 1-100% of the flow rate. A constant flow-rate of 1.31 L/h, related to mean precipitation in this region, was used in the leaching experiments, on approximately 8.4 kg of tailings and 11.5 of mining wastes, which packed the column. The filtration velocity obtained was of $2.05 \cdot 10^{-5}$ m/s, and the pore velocity was of $9.35 \cdot 10^{-5}$ for tailings and $6.64 \cdot 10^{-5}$ for mining wastes. In addition, the pore volume reached in the column experiments:

$$T_a = v \cdot t \cdot L^{-1}$$

Where T_a is the number of pore volumes, v the pore velocity (m/s), t is the time of leaching (s) and L the column length (m). The final T_a was 5.46 pore volumes for tailings and 4.62 for mining wastes, indicating a time period which may be considered as representative.

Water samples were quickly sealed for anion analysis and filtered, acidified and sealed for metal analysis. Fluids were analyzed at Actlabs (Ontario, Canada) using IC to determine the dominant anions and using ICP-MS to analyze the following elements: Li, Na, Mg, Al, Si, K, Ca, Sc, Ti, V, Cr, Mn, Fe, Co, Ni, Cu, Zn, Ge, As, Se, Br, Rb, Sr, Y, Zr, Ag, Cd, Sn, Sb, Te, I, Cs, Ba, Hg, Pb, and REE. Results were compared to the reference sample NIST 1640 to confirm accuracy.

Hydrogeochemical analyses of leachates were performed using the PHREEQC (Parkhurst and Appelo 1999) numerical code (version 3.0.6-7757) to evaluate the speciation of dissolved constituents and calculate the saturation state of the effluents. The MINTEQ thermodynamic database was used for chemical equilibrium calculations and the thermodynamic data of Preis and Gamsjäger (2001).

Results and discussion

Physical parameters

The results of grain size measurements showed that equivalent diameter of tailings and mining wastes were 1.5 and 6 mm, respectively. The bulk density and porosity of tailings gave a result of 1.29g/cm^3 and 0.22, respectively, while mining wastes showed a bulk density of 2.1 g/cm^3 and a porosity of 0.31.

Mineralogy and geochemistry of ore, mine wastes and tree leaves

The mineralogical composition of solid samples is given in Table 1. Quartz, fluorite, barite, calcite, galena, sphalerite, pyrite, albite, biotite, muscovite, and kaolinite were detected by XRD, binocular microscope and visual inspection.

Mining wastes sample from the Osor sector (EM-1 in Table 2) contained high amounts of Pb ($>5000\text{ mgkg}^{-1}$) due to the presence of argentiferous galena and high concentrations of Na, K, and Mg from silicates and possibly jarosite. The high content of Zn (11300 mgkg^{-1}) and Cd (24.9 mgkg^{-1}) could be associated with sphalerite, whereas the elevated concentration of Sb may be linked to galena or undetected sulfosalts. The Osor flotation tailings sample (TOS in Table 2) contains high amounts of Al, Ba, and Sr due to concentration of gangue material in the flotation processes. Soil samples in the Osor area were comprised of alluvial soils (OS-6, OS-7, OS-10) and a stream sediment (OS-9), collected close to the water sampling locations (Fig. 1), and a sample of the sediment deposited in the Coral adit (sample OS-8, Table 2). The analysis of sampled soils and sediments revealed high concentrations of As, Ba, Cd, Co, Sb, Pb, and Zn (Table 2) which are above the metal concentrations of the Catalonian soil intervention values.

Sample OS-8, associated with mine water in the Coral adit contained relatively high amounts of As (121 mgkg^{-1}), Co (2540 mgkg^{-1}), Ni (506 mgkg^{-1}), Pb (3230 mgkg^{-1}), and Zn (71000 mgkg^{-1}) compared to most other samples and the highest amounts of Fe (7.75 %) and Mn (4.93 %) of all samples. The amorphous character of this solid based on XRD suggests it may be composed of Fe and Mn oxy-hydroxides, which have sorbed high amounts of metals, and possibly hydrozincite ($\text{Zn}_5(\text{OH})_6(\text{CO}_3)_2$) or an amorphous hydrated ZnCO_3 predecessor. Thus, the presence of As in the Coral adit sediment may be associated with Fe oxy-hydroxides and the sorption of this metalloid by the amorphous oxy-hydroxides. In the alluvial soils from the Osor area, only Ba, Pb, and Zn showed elevated concentrations in the sample OS-6 (Table 2), which, possibly, was collected above an old mine wastes impoundment.

Tree leaf compositions reveal that all sampled plants accumulate some metals (samples O-6 to O-10 in Table 2), and the metal concentration in the samples collected from the Osor area exceed the concentrations detected in the reference sample (O-0) located in an uncontaminated area near the Ter river, close to the studied area. The recognition of accumulator plants was based on a comparison of the metal concentration in the plant to the metal concentration in the soil or the bioaccessible metal in the soil, using extraction techniques such as diethylene triamine pentaacetic acid (Lottermoser 2011). The samples analyzed indicated an accumulation of Au and Zn in the leaves compared to the mean chemical composition of these

metals in the Osor soils (Table 2). This comparison don't include the sediment of the Coral adit (sample OS-8) or the contaminated soil sample OS-6.

The mobility of Zn within plant varies depending on species, although Zn is likely to concentrate in mature leaves and in roots (Kabata-Pendias and Mukherjee 2007). Thus, plants cultivated close to mining works may contain elevated amounts of Zn (13.9, 66.9 mg.kg⁻¹) (Kabata-Pendias and Mukherjee 2007). However, Zn concentration in tree leaves of black poplar in the studied area reaches values of 146–1220 mg.kg⁻¹, which is above the content which may stop the photosynthesis (178 mg.kg⁻¹). The accumulation of Zn in these plants may be explained by the low content of several soil parameters which may control the behavior of Zn in soils, such as phosphates, oxides and organic matter that may contribute to the metal retention in soils. Also, in the old Pb-Zn mining areas of Aran Valley (Pyrenees, NE Spain) was detected the enrichment of several plants for Zn and Ni (Marques et al. 2003).

Tables 1 and 2

Waters

Dissolved concentrations of major and minor components showed a considerable difference between the samples obtained during the summer and winter sampling campaigns (Table 3 and 4). The hydrogeochemistry of the Osor water samples and mine water showed that superficial waters are of a dominant HCO₃-Ca character, while mine water samples of the Coral adit (OS-8, OS-11) showed a dominant HCO₃, SO₄-Ca composition (Fig. 2). The composition of these waters also shows a possible close relationship between the Coral mine water adit (OS-8 and OS-11 samples) and the Coral spring (OS-10 samples; Tables 3 and 4) suggesting that weathering of similar materials may be the origin of the hydrogeochemical composition of these waters. Mine water samples showed the greater metallic content and an increase in average alkalinity from 40–45 mg/L to 290–377 mg/L (as HCO₃⁻), which could be indicative of sulphide oxidation and subsequent acid neutralization via carbonate dissolution.

Analytical results of water samples showed that some samples exceed the EPDWR (European Primary Drinking Water Regulations) for Mn, Fe, Ni, Pb, F and SO₄ (Tables 3 and 4). Fe and Mn clearly exceeded the EPDWR (50 and 200 µg/L, respectively), showing the highest concentrations in mine water samples (OS-8 and OS-11). Pb is possibly the contaminant of greater environmental concern since three samples (OS-6 and OS-11) have a concentration above the limit established by EPDWR (10 µg/L). Although Pb is relatively immobile in soils and groundwater because of its tendency to be adsorbed by Fe and Mn oxyhydroxides, and because of the low solubility of Pb minerals (Pb sulphate and hydroxycarbonate) still, high Pb concentrations were measured in some samples. These Pb concentrations are similar to those detected in the old Pb mining district of La Carolina, Southern Spain (Hidalgo et al. 2010), where mine water showed neutral pH and Pb concentrations comprised between 0.6 and 850 µg/L. Also, the mobility of Pb in other abandoned mining areas, where waters showed a circum-neutral pH and high contents of Pb, was associated to the stability of PbCO₃⁰ species, under these pH conditions (Cidu et al. 2009), which is also stable under the observed conditions of the studied area.

Also, high concentrations of F were detected (1.9 and 2.31 mg/L) in most impacted waters, above the EPDWR (1.5 mg/L), associated to the nature of ore deposits. Zinc was the dominant base metal in sampled waters, ranging between 34.4 and 2810 µg/L and reaching >250 and 2810 µg/L in mine waters.

The variations in dissolved metal concentrations with pH showed that base metals such as Cd and Cu tended to increase with decreasing pH. However, Cd showed significant concentrations at neutral pH, especially in the leachate samples. Ni concentrations showed a similar pattern, reaching higher concentrations at low pH and associated with the groundwater and leachate samples. In mine water samples, Zn reached 2800 µg/L, showing high concentrations under neutral pH conditions (7.08-7.68). Moreover, mine waters showed a direct relationship between high Zn and Cd contents (Table 4).

Oxyanion-forming elements such as As showed significant concentrations under neutral-alkaline pH conditions, whereas the lower concentrations were associated with water samples with low pH (groundwater) and some samples with an elevated pH (superficial water samples). In general, the low concentration of As in waters may be associated with lower percentages of arsenical pyrite and arsenopyrite in the minerals exploited, and with the possible adsorption onto Fe oxyhydroxides (Navarro and Domènech 2010).

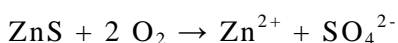
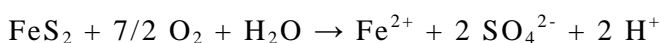
Tables 3 and 4

Mine water samples (OS-8 and OS-11) showed high concentrations of Ca (116–189 mg/L), HCO₃ (290–377 mg/L), SO₄ (156–288 mg/L), and an elevated pH (7.08-7.68), which may indicate the calcite dissolution through the Coral adit. The elevated concentration of SO₄²⁻ can be associated to sulphide oxidation, although could be possible the gypsum dissolution despite their absence in XRD analysis. Also, the elevated concentrations of Mn (0.19-1.8 mg/L) and Zn (up to 2.8 mg/L) suggest the dissolution of sphalerite and Mn oxides.

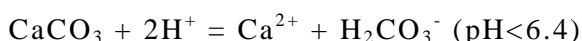
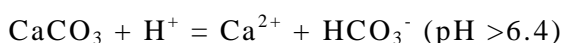
Fig. 2

The possible main hydrochemical reactions associated to sulphide oxidation and carbonate dissolution are the following:

(1) Pyrite and sphalerite oxidation.



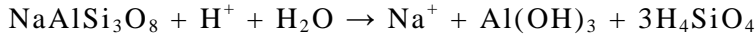
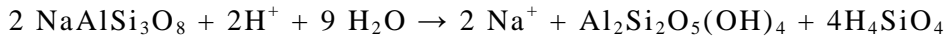
(2) Calcite dissolution (Lottermoser 2003).



Moreover, mine water showed elevated concentrations of some cations, such as Na (31.4-42.5 mg/L), Mg (18.0-28.0 mg/L), and K (4.5-6.2 mg/L), above their concentrations in surface water and springs (Table 3). The weathering of some detected silicates (albite and muscovite) may also explain the high pH detected. Progress of the feldspar alteration reactions changes the activities of

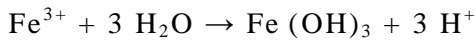
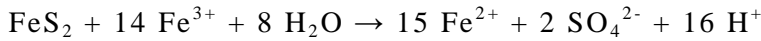
the dissolved solutes: Ca^{2+} , Na^+ , K^+ , H^+ , $\text{SiO}_{2(\text{aq})}$, thus albite and other aluminosilicates detected will not be stable in these waters and must dissolve:

(3) Silicate (albite) dissolution (Appelo and Postma 1996).



Moreover, gibbsite [$\text{Al}(\text{OH})_3$] may be a weathering product of silicates, and dissolved Al in waters may be associated with gibbsite dissolution. These neutralization processes and the scarce quantity of pyrite may explain the elevated pH of waters and leachates, and, to a lesser extent, the mobility of metals such as Zn, and the possible immobilization of Fe in mine waters, resulting in low concentrations of Fe at mine waters (samples OS-8 and OS-11 in Table 3). Also, precipitation of Fe oxy-hydroxides was observed at the Coral portal because of the possible oxidation and precipitation of Fe. These reactions are the following:

(4) Fe^{2+} oxidation and oxy-hydroxides precipitation (Stumm and Morgan 1996).



Leaching experiments

In order to evaluate the factors that control the mass-transfer in the column experiments and the proximity to equilibrium conditions the Damköhler numbers were calculated. The Damköhler numbers express the rate of reaction relative to the advection or fluid flow rate, and values over 10 indicate near equilibrium conditions (Wehrer and Totsche 2003, 2005, 2008). The Damköhler number is expressed by (Grathwohl 2014):

$$D_a = x_{\text{column}} \cdot X_s^{-1}$$

Where x_{column} is the length characteristic of fluid domain (column length filled with porous material) and X_s is the distance traveled after 63.2 % of the equilibrium is achieved (Grathwohl 2014). X_s may be evaluated from:

$$X_s = v \cdot \varepsilon / \{ (S_h \cdot D_{\text{aq}} / d_e^2) \cdot (1 - \varepsilon) \cdot 6 \}$$

Where v is the pore velocity, ε is the porosity, S_h is the Sherwood Number, D_{aq} is the diffusion coefficient, d_e is the equivalent diameter of porous media and the constant 6 is associated to spherical grains. Using Sherwood Numbers comprised between 7 and 10, the Damköhler number of the column experiments reaches values above 10, indicating a situation close to equilibrium conditions. In addition, the equilibrium time in the column experiments was evaluated from:

$$T_{eq} = (x_{column}/v) \cdot \{R \cdot [1 - (X_S/x_{column})]\}$$

Where T_{eq} is the equilibrium time and R is the retardation factor. For a retardation factor of 2, we find a T_{eq} of 131.5 min for tailings and 151.1 for mining wastes. These results indicated that equilibrium may be reached during the leaching tests.

Results of leaching experiments are shown in Table 5 and Figs. 3 and 4. The continuous decrease of concentrations during steady state flow (Figs. 3 and 4) indicates that the metal concentrations in the leachate are rather controlled by availability than solubility of pure mineral phases (Wehrer and Totsche 2008). The evolution of Pb and Ni show a continuous decrease of concentration during experiments (Table 5), the mining wastes (samples EM-1 to EM-6) reaching concentrations above the maximum contaminant level of leachates for inert solid wastes (150 $\mu\text{g/L}$). The evolution of Zn in tailings and mining wastes (Fig. 3) showed, likewise concentrations above the maximum contaminant level for inert solid wastes (1200 $\mu\text{g/L}$). The release of Cd in mining wastes leaching (Table 5) showed the continuous decrease of concentration, which reached values clearly above the maximum contaminant level (20 $\mu\text{g/L}$).

Leachates from Osor mining wastes (Table 5) showed pH values between 6.66 and 7.50 and electrical conductivity values comprised between 260 and 470 $\mu\text{S/cm}$. The most elevated values of electrical conductivity were associated to Osor tailings leachates (TOS-1 and TOS-2). Also, the results of the leaching experiments showed that the most released metal was Zn, which showed concentrations of 0.5-2.3 and 4.5-42.0 mg/L in tailings and mining wastes, respectively (Table 5), which coincides with the most abundant metal in waters.

Table 5 Fig. 3 and 4

Geochemical modeling

Aqueous speciation and saturation state

PHREEQC was used on summer-water samples because were, generally, the most mineralized fluids and showed that the most abundant species of Fe are Fe^{2+} and FeSO_4 . The aqueous speciation of Pb was dominated by PbCO_3^0 with other species (Pb^{2+} , PbHCO_3^+ , PbOH^+) lower by one and two orders of magnitude, in a similar proportion to other Pb contaminated areas (Navarro and Martínez 2010). The aqueous speciation of Zn showed that Zn^{2+} is the most abundant species. The remaining species (ZnSO_4 , ZnCO_3 , $\text{Zn}(\text{CO}_3)_2^{2-}$) are generally lower by one and two orders of magnitude.

The calculated saturation indexes (SI) (Table 6) showed that most waters were saturated with respect to ferrihydrite and goethite, with the exception of EM-1 leachate. Mine water sample (OS-11) and Grevolosa Creek (OS-6) were near equilibrium. On the other hand, waters and leachates were undersaturated with regards to Fe sulfate minerals and gypsum, with the exception of water sample OS-11 (Coral adit drainage) which showed a value close to equilibrium for jarosite, and TOS-1 leachate (leachate from Osor tailings), which showed oversaturation with regards to jarosite, jarosite-Na, and close to equilibrium with regards to gypsum. This is probably associated to the leaching method, which is far from equilibrium for some slowly reacting mineral phases.

As for Pb and Zn minerals, all the water samples and leachates were undersaturated with anglesite, cerussite and smithsonite. Only the leachates EM-1 and TOS-1 (Table 6) showed SI values near equilibrium with respect to cerussite, which suggests the possible control of dissolved Pb by PbCO_3 . In addition, mine drainage waters (OS-8 and OS-11) and EM-1 leachates were close to equilibrium with respect to smithsonite, which may indicate control of dissolved Zn by this mineral phase. However, a possible solid phase sink for Zn may be hydrozincite ($\text{Zn}_5(\text{OH})_6(\text{CO}_3)_2$) which could precipitate via an amorphous hydrated ZnCO_3 predecessor (Younger 2000). Thus, mine water samples from the Coral adit were saturated with respect to hydrozincite or near the equilibrium (OS-11) with respect to $\text{ZnCO}_3 \cdot \text{H}_2\text{O}$ (Table 6), although have not been found crystalline Zn-minerals in the Coral adit sediment.

Furthermore, carbonate minerals calcite, dolomite, and siderite were undersaturated in almost all the samples, showing values near to equilibrium in leachates (TOS-1) and mine drainage waters (OS-8 and OS-11 in Table 6). Also, the SI of gibbsite, which showed in all the samples with the exception of leachates, show values close to equilibrium, suggesting this mineral phase controls the concentrations of dissolved Al. The representation of water samples in the (Ca+Mg) vs. ($\text{HCO}_3 + \text{SO}_4$) scatter diagram show that ionic concentrations falling above the equiline may result from carbonate weathering, while those falling along the equiline are due to both carbonate and silicate weathering (Elango and Kannan 2007). Thus, most of the sample points lie along the equiline scatter diagram of the Osor water samples, which could indicate the weathering of carbonates and silicates (Fig. 5).

Eh-pH conditions were consistent with these data, showing that under the Eh-pH conditions of leachates and waters, the most stable species for Fe, Pb, and Zn were oxy-hydroxides of Fe, cerussite, and Zn^{2+} .

Table 6 and Fig. 5

Evaluation of metal mobilization

Metal mobilization from the main potential source: the Coral adit, was evaluated from flow-rate measurements and contaminant concentrations of Coral adit water samples. The main contaminant spill from the Coral adit to the Osor creek stream was evaluated using the mathematical expression of contaminant mass-flow:

$$M = \int C_0 V n \, dA, \text{ where:}$$

M : contaminant mass-flow (kg/day).

C_0 : mean contaminant concentration (kg/m³).

V: volume of mine water (m³).

n : elemental vector.

dA: differential surface element (m²).

$\int V n \, dA$: adit flow-rate (m³/day).

The concentrations of samples OS-8 and OS-11 (Tables 3 and 4) were used in order to evaluate the seasonal contaminant mass-flow, by evaluating the mean

concentration of samples OS-8(S) and OS-11(S) for summer production. The flow-rate of Coral adit was evaluated from discrete measures, thus, the measured flow-rate of the Coral adit showed the following values: 880 m³/day (summer 2009), 296.2 m³/day (summer 2010), 1100.6 m³/day (autumn 2010) and 1073 m³/day (winter 2010) with a mean value of 837 m³/day, equivalent to 305,733 m³/year.

The mobilization of Mn, Fe, and Ni is shown in Fig. 6, where Mn production reached values near 0.8 kg/day in summer and autumn, while Fe and Ni were mobilized at low quantity. The production of Zn, Cd, Pb and SO₄ is shown in Fig. 7, indicating a greater Zn production at 1–3 kg/day for summer and autumn. The mobilization of SO₄⁻² was very high, with a calculated production of 137–188 kg/day. However, the mobilization of Cd and Pb is low, although Pb production may reach 0.006 kg/day in summer period.

Figs. 6 and 7

Conclusions

The old mining activities in the Osor area have contaminated soils, sediments, groundwater, and surface water in extensive zones, in spite of the neutral character of leachates and mine water generation. Mining wastes from the Osor sector contained high amounts of Pb (>5000 mgkg⁻¹), Zn (11300 mgkg⁻¹) and Cd (24.9 mgkg⁻¹) which are possibly associated with sphalerite. The Osor tailings sample had high concentrations of Al, Ba, and Sr due to the composition of gangue and soil. Sediment samples revealed high concentrations of As, Ba, Cd, Co, Sb, Pb, and Zn, which are above the metal concentration of the Catalonian soil intervention values.

Mine water samples showed high concentrations of Ca (116–189 mg/L), HCO₃ (290–377 mg/L) and SO₄ (156–288 mg/L). The origin of dissolved SO₄⁻² may be associated to sulphide oxidation, although gypsum dissolution could be thermodynamically possible because mine waters and superficial waters are undersaturated with respect to this mineral, however gypsum have not been found in ore and mine wastes samples. Besides mine water showed an elevated pH (7.08-7.68) which may indicate calcite dissolution through the Coral adit. In addition, the elevated concentrations of Mn (0.19-1.8 mg/L) and Zn (>0.25-2.8 mg/L) suggest the dissolution of sphalerite and Mn oxides. Moreover, mine water showed elevated concentrations of some cations such as Na (31.4-42.5 mg/L), Mg (18.0-28.0 mg/L), and K (4.5-6.2 mg/L) above their concentrations in surface water.

Column leaching experiments showed that the metal concentrations in the leachate are rather controlled by availability than solubility of mineral phases. The most released metal was Zn, which showed concentrations of 0.5-2.3 and 4.5-42.0 mg/L in tailings and mining wastes, respectively, which coincides with the most abundant metal in waters.

Geochemical modeling of mine waters and leachates indicated that some waters were close to equilibrium with respect to smithsonite, which may indicate control of dissolved Zn by this mineral phase. However, another possible solid phase sink for Zn could be hydrozincite (Zn₅(OH)₆(CO₃)₂) since mine water showed saturation with respect to this mineral.

The flow rate of the Coral adit showed an inverse relationship with electrical conductivity and some dissolved cations (Na, Mg, K, Mn, Co, Cd and Pb), possibly, because the dilution effect of increasing flow rate. The main environmental concern in this area is the mobilization of Zn and SO_4^{2-} by the Coral adit, estimated as 0.26-3.0 kg/day and 137.6-188.1 kg/day, respectively. It is worth noting from these data that there is a significant quantity of Zn and SO_4^{2-} , which the Coral adit sends to the Osor creek, and therefore pollutes these superficial waters.

Acknowledgements

The research was supported by the Consolidated Research Group on Economic and Environmental Geology and Hydrology at the University of Barcelona (UB), with financial support from the Catalan Agency for the Administration of University and Research Grants (AGAUR) (project SGR2005). The authors wish to thank the anonymous reviewers for the review of the manuscript.

References

- Al TA, Martin CJ, Blowes DW (2000) Carbonate-mineral/water interactions in sulfide-rich mine tailings. *Geochim Cosmochim Acta* 64 (23): 3933–3948
- Appelo CAJ, Postma D (1996) *Geochemistry, groundwater and pollution*. Balkema, Rotterdam
- Blowes DW, Ptacek CJ (1994) Acid-neutralization mechanisms in inactive mine tailings. In: Jambor JL, Blowes DW (eds), *The Environmental Geochemistry of Sulfide Mine-Wastes*. Mineralogical Assoc of Canada Short Course Handbook 22, p 271–292
- Blowes DW, Jambor JL, Hanton-Fong CJ (1998) Geochemical, mineralogical and microbiological characterization of a sulphide-bearing carbonate-rich gold-mine tailings impoundment, Jouetl, Québec. *Appl Geochem* 13: 687–705
- Canals A, Cardellach E (1997) Ore lead and sulphur isotope pattern from the low-temperature veins of the Catalonian Coastal Ranges (NE Spain). *Miner Depos* 32: 243–249
- Cardellach E, Canals A, Tritlla J (1990) Late and post-Hercynian low temperature veins in the Catalonian Coastal Ranges. *Acta Geologica Hispanica* 25: 75–81
- Cidu R, Bidau R, Fanfani L (2009) Impact of past mining activity on the quality of groundwater in SW Sardinia (Italy). *J Geochem Explor* 100: 125–132
- Durán H. (1990). El Paleozoico de les Guillerries. *Acta Geologica Hispanica* 25 (1–2): 83–103
- Elango L, Kannan R (2007) Rock-water interaction and its control on chemical composition of Groundwater. In: Sarkar D, Datta R, Hannigan R (eds) *Developments in Environmental Science*, Vol. 5, Elsevier, p 229–243
- Enrique P (1990) The Hercynian intrusive rocks of the Catalonian Coastal Ranges (NE Spain). *Acta Geologica Hispanica* 25: 39–64

- Ezekwe IC, Ezekwe AS, Chima GN (2013) Metal Loadings and Alkaline Mine Drainage from Active and Abandoned Mines in the Ivo River Basin Area of Southeastern Nigeria. *Mine Water Environ* 32: 97–107
- Grathwohl P (2014) On equilibration of pore water in column leaching tests. *Waste Management* 34: 908–918
- Heikkinen PM, Räsänen ML, Johnson RH (2009) Geochemical Characterization of Seepage and Drainage Water Quality from Two Sulphide Mine Tailings Impoundments: Acid Mine Drainage versus Neutral Mine Drainage. *Mine Water Environ* 28: 30–49
- Heikkinen PM, Räsänen ML (2009) Trace metal and As solid-phase speciation in sulphide mine tailings-Indicators of spatial distribution of sulphide oxidation in active tailings impoundments. *Appl Geochem* 24: 1224–1237
- Hidalgo MC, Rey J, Benavente J (2010) Hydrogeochemistry of abandoned Pb sulphide mines: the mining district of La Carolina (southern Spain). *Environ Earth Sci* 61: 37–46
- Jang M, Kwon H (2011) Pilot-scale tests to optimize the treatment of net-alkaline mine drainage. *Environ Geochem Health* 33: 91–101
- Jurjovec J, Ptacek CJ, Blowes DW (2002) Acid neutralization mechanisms and metal release in mine tailings: A laboratory column experiment. *Geochim Cosmochim Acta* 66(9): 1511–1523
- Kabata-Pendias A, Mukherjee AB (2007) *Trace Elements from Soil to Human*. Springer, Berlin
- Lee JY, Choi JC, Lee KK (2005) Variations in heavy metal contamination of stream water and groundwater affected by an abandoned lead-zinc mine in Korea. *Environ Geochem Health* 27: 237–257
- Lindsay MBJ, Condon PD, Jambor JL, Lear KG, Blowes DW, Ptacek CJ (2009) Mineralogical, geochemical, and microbiological investigation of a sulfide-rich tailings deposit characterized by neutral drainage. *Appl Geochem* 24: 2212–2221
- Lottermoser B (2003). *Mine Wastes*. Springer, Berlin
- Lottermoser B (2011) Colonisation of the rehabilitated Mary Kathleen uranium mine site (Australia) by *Calotropis procera*: Toxicity risk to grazing animals. *J Geochem Explor* 111: 39–46
- Marques AF, Queralt I, Carvalho ML, Bordalo M (2003) Total reflection X-ray fluorescence and energy-dispersive X-ray fluorescence analysis of runoff water and vegetation from abandoned mining of Pb-Zn ores. *Spectrochimica Acta Part B* 58: 2191–2198
- Munson BR, Okiishi TH, Huebsch WW (2009) *Fundamentals of Fluid Mechanics*. Hoboken, NJ
- Navarro A, Collado D, Carbonell M, Sánchez, J.A. (2004). Impact of mining activities on soils in a semi-arid environment: Sierra Almagrera district, SE Spain. *Environmental Geochemistry & Health*, 26, 383–393.

- Navarro A, Cardellach E (2009) Mobilization of Ag, Heavy metals and Eu from the waste deposit of Las Herrerías mine (Almería, SE Spain). *Environ Geol* 56 (7): 1389–1404
- Navarro A, Martínez F (2010) Evaluation of Metal Attenuation from Mine Tailings in SE Spain (Sierra Almagrera): A Soil-Leaching Column Study. *Mine Water Environ* 29: 53–67
- Navarro A, Domènech LM (2010) Arsenic and metal mobility from Au mine tailings in Rodalquilar (Almería, SE Spain). *Environ Earth Sci* 60: 121–138
- Parkhurst DL, Appelo CAJ (1999) User's Guide to PHREEQC (version 2)-a computer program for speciation, batch-reaction, one-dimensional transport, and inverse geochemical calculations, USGS Water-Resources Investigations Report 99-4259, 312 pp
- Piqué A, Canals A, Grandia F, Banks DA (2008) Mesozoic fluorite veins in NE Spain record regional base metal-rich brine circulation through basin and basement during extensional events. *Chem Geol* 257: 139–152
- Plante B, Benzaazoua M, Bussière B (2011) Predicting Geochemical Behaviour of Waste Rock with Low Acid Generating potential Using Laboratory Kinetic Tests. *Mine Water Environ* 30: 2–21
- Plumlee GS, Smith KS, Montour MR, Ficklin WH, Mosier EL (1999) Geologic controls on the composition of natural waters and mine waters. In: Filipek LH, Plumlee GS (eds) *The Environmental Geochemistry of Mineral Deposits. Part B: Case Studies and Research Topics. Reviews in Economic Geology*, vol 6B, Chelsea, MI, USA, p 373–432
- Preis W, Gamsjäger H (2001) (Solid+solute) phase equilibria in aqueous solution. XIII. Thermodynamic properties of hydrozincite and predominance diagrams for (Zn²⁺+H₂O+CO₂). *J Chem Thermodynamics* 33: 803–819
- Reche J, Martínez FJ (2002) Evolution of bulk composition, mineralogy, strain style and fluid flow during an HT-LP metamorphic event: sillimanite zone of the Catalan Coastal Ranges Variscan basement, NE Iberia. *Tectonophysics* 348: 111–134
- SAIC (2003) An Assessment of laboratory leaching Tests for predicting the Impacts of Fill Material on Ground Water and Surface Water Quality. Toxic Cleanup Program, Olympia, Washington
- Seal RR, Foley NK (2002) Progress on Geoenvironmental Models for Selected Mineral Deposit Types. U.S. Geological Survey Open-File Report 02-195
- Seal RR, Hammarstrom JM (2003) Geoenvironmental models of mineral deposits: examples from massive sulfide and gold deposits. In: Jambor JL, Blowes DW, Ritchie AIM (eds) *Environmental Aspects of Mine Wastes. Mineralogical Association of Canada, Short Course Series 31*
- Seal RR, Hammarstrom JM, Johnson AN, Piatak NM, Wandless GA (2008) Environmental geochemistry of a Kuroko-type massive sulfide deposit at the abandoned Valzinco mine, Virginia, USA. *Appl Geochem* 23: 320–342
- Stumm W, Morgan JJ (1996) *Aquatic Chemistry. Chemical Equilibria and Rates in Natural Waters*. Wiley, New York

Viladevall M, Fondevilla M, Puigserver D, Carmona JM, Cortés A, Navarro A (2007) Poplar trees used for the detection of hazardous elements: case history of the Ebro, Llobregat and Ter valleys (NE, Spain). In: Loredó J (ed) Proceedings of the 23rd International Geochemistry Symposium (IAGS), pp 145-146

Wehrer M, Totsche KV (2003) Detection of non-equilibrium contaminant release in soil columns: delineation of experimental conditions by numerical simulations. *Journal of Plant Nutrition and Soil Science* 166: 475–483

Wehrer M, Totsche KV (2005) Determination of effective release rates of polycyclic aromatic hydrocarbons and dissolved organic carbon by column outflow experiments. *European Journal of Soil Science* 56: 803–813

Wehrer M, Totsche KV (2008) Effective rates of heavy metal release from alkaline wastes-Quantified by column outflow experiments and inverse simulations. *J Contam Hydrol* 101: 53–66

Younger PL (2000) Nature and practical implications of heterogeneities in the geochemistry of zinc-rich, alkaline mine waters in an underground F-Pb mine in the UK. *Appl Geochem* 15: 1383–1397

TABLES

Table 1.- Main mineral phases identified in the contaminated soils and mine wastes. M: major, m: minor, T: trace.

| | | |
|---|---|--|
| Sample EM-1 | | |
| Silicates | | |
| Quartz | m | SiO ₂ |
| Albite | M | Na AlSi ₃ O ₈ |
| Muscovite | m | KAl ₂ (AlSi ₄) ₄ O ₁₀ (OH,F) ₂ |
| Biotite | m | KMg _{1.5} Fe _{1.5} AlSi ₃ O ₁₀ (OH) ₂ |
| Kaolinite | T | Al ₄ (Si ₄ O ₁₀) (OH) ₈ |
| Carbonates | | |
| Calcite | M | CaCO ₃ |
| Sulphates, sulphides and fluorides | | |
| Barite | m | BaSO ₄ |
| Galena | m | PbS |
| Sphalerite | M | ZnS |
| Pyrite | T | FeS ₂ |
| Fluorite | M | CaF ₂ |
| Sample TOS | | |
| Quartz | M | SiO ₂ |
| Calcite | M | CaCO ₃ |
| Barite | m | BaSO ₄ |
| Kaolinite | T | Al ₄ (Si ₄ O ₁₀) (OH) ₈ |

Table 2.- Concentrations of metals and metalloids in contaminated soils, ore samples, mine wastes, and vegetation. D: depth of the samples, sup: superficial. CAL(*): The Catalanian soil intervention values (industrial use). EM-1: mining wastes, TOS: tailings. O-0 (control sample) to O-10: tree leaf of black poplar. ND: not determined. DL: detection limit.

| Element | D | COORDINATES | Al | Ag | As | Au | Ba | Bi | Ca | Cd | Co |
|------------|-----|-----------------|------|-------|-------|-------|-------|-------|------|-------|-------|
| Unit | m | UTM | % | mg/kg | mg/kg | µg/kg | mg/kg | mg/kg | % | mg/kg | mg/kg |
| DL | --- | | 0.01 | 0.3 | 0.01 | 2 | 50 | 2 | 0.01 | 0.3 | 0.1 |
| EM-1 | 0.3 | 466412, 4644083 | 0.61 | 29.9 | 15.2 | 6 | 250 | 0.4 | 29.8 | 24.9 | 6 |
| TOS | 0-2 | 466421, 4644434 | 4.46 | 0.6 | 12.5 | <2 | 5110 | 0.3 | 7.33 | 7.6 | 14 |
| Osor vein | sup | 466468, 4644095 | 0.24 | 66.2 | 164 | 32 | 2190 | <2 | 21.4 | 68.5 | 15 |
| soil OS-6 | 0.3 | 466209, 4644283 | 6.48 | 3.5 | 5.7 | <2 | 2200 | <2 | 4.62 | 11.5 | 9 |
| soil OS-7 | 0.3 | 466182, 4644259 | 7.4 | <0.3 | 3 | <2 | 860 | <2 | 0.61 | <0.3 | 6 |
| soil OS-8 | 0.3 | 467203, 4644270 | 1.31 | 2.7 | 121 | <2 | <50 | 3 | 11.3 | 74.7 | 2540 |
| soil OS-9 | 0.3 | 467240, 4644241 | 7.01 | <0.3 | <0.5 | <2 | 890 | <2 | 0.66 | <0.3 | 6 |
| soil OS-10 | 0.3 | 467215, 4644254 | 7.77 | 0.5 | 6.7 | <2 | 900 | <2 | 0.62 | 0.6 | 10 |
| CAL* | --- | ----- | --- | --- | 30 | --- | 1000 | --- | --- | 55 | 90 |
| O-0 | --- | 470112, 4645612 | ND | <0.3 | 0.6 | 5.7 | 50 | ND | 4.6 | ND | 3.4 |
| O-6 | --- | 466203, 4644256 | ND | <0.3 | 0.3 | 5.3 | 203 | ND | 4.7 | ND | 1.1 |
| O-7 | --- | 466181, 4644221 | ND | <0.3 | 0.4 | 17.6 | 173 | ND | 3.5 | ND | 1 |
| O-8 | --- | 467147, 4644440 | ND | <0.3 | 0.3 | 4.4 | 45 | ND | 3.8 | ND | 1 |
| O-9 | --- | 467282, 4644225 | ND | <0.3 | 0.4 | 5 | 195 | ND | 4.8 | ND | 1.5 |
| O-10 | --- | 467318, 4644207 | ND | <0.3 | 0.5 | 6.1 | 165 | ND | 4.1 | ND | 0.8 |

| Element | Cr | Cu | Ni | Pb | Sb | Se | Sr | V | W | Zn | Hg | Mn | Mo | Fe |
|------------|-------|-------|-------|-------|-------|-------|-------|-------|-------|-------|-------|-------|-------|------|
| Unit | mg/kg | mg/kg | mg/kg | mg/kg | mg/kg | mg/kg | mg/kg | mg/kg | mg/kg | mg/kg | mg/kg | mg/kg | mg/kg | % |
| DL | 0.3 | 1 | 1 | 1 | 0.005 | 0.1 | 1 | 2 | 0.05 | 1 | 0.05 | 1 | 0.05 | 0.01 |
| EM-1 | <2 | 11 | 3 | >5000 | 56.5 | <0.1 | 17 | 4 | <1 | 11300 | 3 | 89 | <1 | 0.35 |
| TOS | 39 | 47 | 18 | 940 | 1 | <0.1 | 105 | 45 | <1 | 2370 | <1 | 684 | 1 | 1.78 |
| Osor vein | 119 | 88 | 31 | >5000 | 208 | <3 | 74 | 15 | <1 | 34000 | 5 | 109 | 1 | 0.96 |
| soil OS-6 | 44 | 24 | 19 | >5000 | 6.1 | <3 | 109 | 48 | <1 | 2730 | <1 | 418 | 2 | 2.54 |
| soil OS-7 | 14 | 9 | 6 | 22 | 0.2 | <3 | 141 | 31 | <1 | 79 | <1 | 322 | <1 | 2.11 |
| soil OS-8 | <2 | 18 | 506 | 3230 | 3.5 | <3 | 103 | 13 | 15 | 71000 | <1 | 49300 | 8 | 7.75 |
| soil OS-9 | 22 | 9 | 8 | 55 | 0.5 | <3 | 136 | 36 | <1 | 114 | <1 | 351 | 2 | 2.01 |
| soil OS-10 | 45 | 19 | 23 | 50 | 0.4 | <3 | 102 | 64 | 4 | 209 | <1 | 519 | <1 | 3.12 |
| CAL* | 1000 | 1000 | 1000 | 550 | 30 | 70 | --- | 1000 | --- | 1000 | 30 | --- | 70 | --- |
| O-0 | 1.8 | 6 | <1 | 1 | 0.06 | 0.4 | 110 | ND | <0.05 | 53 | <0.05 | 61 | 0.7 | 0.09 |
| O-6 | 2.3 | 11 | <1 | 15 | 0.11 | <0.1 | <10 | ND | <0.05 | 974 | 0.35 | 81 | 0.56 | 0.02 |
| O-7 | 1.5 | 5 | <1 | 13 | 0.08 | <0.1 | 120 | ND | <0.05 | 589 | 0.22 | 144 | <0.05 | 0.05 |
| O-8 | 1.1 | 7 | <1 | 4 | 0.06 | <0.1 | <10 | ND | <0.05 | 982 | <0.05 | 75 | <0.05 | 0.01 |
| O-9 | 0.0 | 9 | <1 | <1 | 0.06 | <0.1 | 140 | ND | <0.05 | 146 | 0.3 | 126 | <0.05 | 0.03 |
| O-10 | 1.1 | 6 | <1 | 8 | 0.07 | <0.1 | <10 | ND | <0.05 | 1220 | 0.29 | 31 | 0.32 | 0.01 |

Table 3.- Main metal contents of water samples. ND: not determined. OS-6(S,W,A): Grevolosa creek (summer/winter/autumn), OS-7(S,W,A): Osor creek (summer/winter/autumn), OS-8(S,W,A): Coral mine drainage (summer/winter/autumn), OS-9(S,W,A): Osor creek, downstream mine drainage (summer/winter/autumn), OS-10(S,W,A): Coral spring (summer/winter/autumn), OS-11: Coral mine drainage (summer 2009). EPDWR: European primary drinking water regulations (maximum contaminant level). *: USA National Secondary Drinking Water Regulation. COOR: coordinates. DL: detection limit.

| Symbol | COOR | Na | Mg | Al | K | Ca | Mn | Fe | Co | Ni | Cu | Zn | As | Se | Cd | Ba | Pb |
|-----------|-----------------|-------|-------|------|------|------|------|------|-------|------|------|-------|------|------|------|------|------|
| Unit | | mg/L | mg/L | µg/L | mg/L | mg/L | µg/L | µg/L | µg/L | µg/L | µg/L | µg/L | µg/L | µg/L | µg/L | µg/L | µg/L |
| DL | | 0.005 | 0.001 | 2 | 0.03 | 0.7 | 0.1 | 10 | 0.005 | 0.3 | 0.2 | 0.5 | 0.03 | 0.2 | 0.01 | 0.1 | 0.01 |
| OS-6 (S) | 466209, 4644283 | 10.3 | 4.1 | 6 | 0.9 | 19.8 | 2.4 | 20 | 0.026 | 0.6 | 0.8 | 192 | 0.17 | <0.2 | 0.57 | 32.4 | 13.6 |
| OS-6 (W) | 466209, 4644283 | 7.72 | 2.5 | 37 | 0.7 | 11.9 | 2.0 | 30 | 0.05 | 0.5 | 1.5 | 55.6 | 0.15 | <0.2 | 0.14 | 20.2 | 3.63 |
| OS-6 (A) | 466209, 4644283 | 8.74 | 3.7 | 5 | 1 | 19.6 | 6 | 70 | 0.15 | 0.7 | 2.5 | 443 | 0.17 | <0.2 | 1.19 | 36.8 | 36.7 |
| OS-7 (S) | 466182, 4644259 | 18.4 | 5.6 | 15 | 1.9 | 26.1 | 57.9 | < 10 | 0.05 | 0.7 | 2 | 34.4 | 0.58 | <0.2 | 0.17 | 108 | 0.72 |
| OS-7 (W) | 466182, 4644259 | 17 | 3.9 | 23 | 1.3 | 19.5 | 14.9 | 50 | 0.05 | 1.1 | 2.1 | 23 | 0.31 | <0.2 | 0.05 | 71.4 | 2.18 |
| OS-7 (A) | 466182, 4644259 | 19.1 | 4.5 | 5 | 2.1 | 33.4 | 10.4 | 80 | 0.05 | 0.8 | 2.8 | 152 | 0.4 | <0.2 | 0.04 | 99.3 | 1.08 |
| OS-8 (S) | 467203, 4644270 | 34.9 | 19.8 | 4 | 5.1 | 134 | 879 | < 10 | 21.8 | 19.4 | 0.3 | 2800 | 0.6 | 0.3 | 2.47 | 39.9 | 2.61 |
| OS-8 (W) | 467203, 4644270 | 31.4 | 18 | 6 | 4.5 | 116 | 193 | <10 | 3.66 | 15.1 | 0.6 | >250 | 0.47 | 0.3 | 1.67 | 36.4 | 1.14 |
| OS-8 (A) | 467203, 4644270 | 28.7 | 16.4 | 3 | 4.3 | 135 | 749 | 240 | 20.1 | 17.9 | 2.8 | 2810 | 0.42 | 0.4 | 1.73 | 29.8 | 1.92 |
| OS-11 (S) | 467203, 4644270 | 42.5 | 28 | 49 | 6.2 | 189 | 1860 | 440 | 53.2 | 38.7 | 10.2 | 2800 | 2.2 | <0.2 | 3.05 | 29.4 | 19.4 |
| OS-9 (S) | 467240, 4644241 | 19.6 | 7.6 | 11 | 2.3 | 42.2 | 141 | 20 | 2.33 | 3.6 | 2.3 | 1000 | 0.49 | <0.2 | 0.39 | 90.8 | 1.69 |
| OS-9 (W) | 467240, 4644241 | 15.5 | 3.8 | 44 | 1.3 | 19.8 | 36.3 | 150 | 0.62 | 1.2 | 2.6 | >250 | 0.32 | <0.2 | 0.13 | 62 | 3.85 |
| OS-9 (A) | 467240, 4644241 | 21.8 | 8.9 | 5 | 2.7 | 74.2 | 226 | 90 | 5.61 | 5.9 | 2.5 | 1040 | 0.42 | <0.2 | 0.54 | 69.4 | 1.39 |
| OS-10 (S) | 467215,4644254 | 10 | 3.5 | 15 | 1.1 | 14 | 2.7 | < 10 | 0.034 | 0.4 | 1.2 | 25.3 | 0.14 | <0.2 | 0.05 | 41.8 | 0.85 |
| OS-10 (W) | 467215,4644254 | 9.74 | 3.6 | 16 | 1.3 | 14.2 | 10.6 | 70 | 0.28 | 0.7 | 1.7 | >250 | 0.26 | <0.2 | 0.06 | 42.5 | 2.46 |
| OS-10 (A) | 467215,4644254 | 11.1 | 2.4 | 6 | 0.7 | 10 | 4.1 | 30 | 0.1 | 0.7 | 2.4 | 157 | 0.07 | <0.2 | 0.04 | 33 | 0.74 |
| EPDWR | --- | 200 | --- | 200 | --- | --- | 50 | 200 | --- | 20 | 2000 | 5000* | 10 | 10 | 5 | --- | 10 |

Table 4.- Main anion contents of water samples. OS-6(S,W,A): Grevolosa creek (summer/winter/autumn), OS-7 (S,W,A): Osor creek (summer/winter/autumn), OS-8 (S,W,A): Coral mine drainage (summer/winter/autumn), OS-9 (S,W,A): Osor creek, downstream mine drainage (summer/winter/autumn), OS-10 (S,W,A): Coral spring (summer/winter)/autumn, OS-11: Coral mine drainage (summer 2009). EPDWR: European primary drinking water regulations (maximum contaminant level). *: as NO₂, **: as NO₃. DL: detection limit.

| Symbol | pH | Eh | EC | F | Cl | NO ₃ (as N) | PO ₄ (as P) | SO ₄ | HCO ₃ (-) | Analytical error (%) |
|-----------|---------|-----|-------|------|------|------------------------|------------------------|-----------------|----------------------|----------------------|
| Unit | pH unit | mV | μS/cm | mg/L | mg/L | mg/L | mg/L | mg/L | mg/L | --- |
| DL | --- | --- | --- | 0.01 | 0.03 | 0.01 | 0.02 | 0.03 | 1 | --- |
| OS-6 (S) | 7.2 | 200 | 145 | 0.2 | 10 | 0.1 | <0.02 | 8.8 | 72 | 3.3 |
| OS-6 (W) | 7.4 | 103 | 78.7 | 0.1 | 6.1 | 0.45 | <0.02 | 8.7 | 45 | 1.3 |
| OS-6 (A) | 7.75 | 103 | 104 | 0.37 | 8.2 | 0.05 | <0.02 | 8.3 | 96 | 1.2 |
| OS-7 (S) | 7.58 | 204 | 204 | 0.2 | 17 | 1.15 | 0.12 | 13 | 96 | 1.0 |
| OS-7 (W) | 8.21 | 60 | 141 | 0.1 | 18 | 1.57 | 0.09 | 11 | 60 | 4.9 |
| OS-7 (A) | 7.77 | 60 | 169 | 0.34 | 30.3 | 1.69 | 0.24 | 13.8 | 112 | 3.4 |
| OS-8 (S) | 7.68 | 197 | 950 | 1.9 | 28 | <0.03 | <0.06 | 180 | 324 | 1.7 |
| OS-8 (W) | 7.38 | -2 | 860 | 2.1 | 26 | <0.02 | <0.04 | 156 | 290 | 6.0 |
| OS-8 (A) | 7.35 | -2 | 563 | 2.31 | 26.9 | <0.03 | <0.06 | 171 | 293 | 0.49 |
| OS-11 (S) | 7.08 | 21 | 1180 | 2.1 | 29 | <0.03 | <0.06 | 288 | 377 | 5.3 |
| OS-9 (S) | 7.58 | 195 | 372 | 0.5 | 17 | 1.33 | 0.16 | 38 | 116 | 4.7 |
| OS-9 (W) | 7.3 | 60 | 159 | 0.2 | 16 | 1.37 | 0.06 | 13 | 61 | 7.9 |
| OS-9 (A) | 7.75 | 60 | 332 | 1.15 | 27.8 | 0.51 | <0.04 | 71.7 | 186 | 3.1 |
| OS-10 (S) | 7.72 | 185 | 123 | 0.2 | 8.2 | 0.17 | <0.02 | 18 | 40 | 1.9 |
| OS-10 (W) | 8.03 | 61 | 104 | 0.2 | 7.2 | 0.3 | <0.02 | 18 | 45 | 0.7 |
| OS-10 (A) | 7.8 | 61 | 60.6 | 0.3 | 8.0 | 0.14 | <0.02 | 18.7 | 41 | 4.0 |
| EPDWR | --- | --- | 2500 | 1.5 | 250 | 50** | --- | 250 | --- | --- |

Table 5a.- Main metal contents of low-mineralized water leaching experiments. TOS-1 to TOS-6: leachate from tailings of Osor dumps (from TOS sample, Table 2). EM-1 to EM-6: leachate from mining wastes of Osor dumps (from EM-1 sample, Table 2). VL: volume of leachate produced at each time interval. t: time. DL: detection limit.

| Symbol | t | VL | pH | Eh | EC | Mn | Fe | Co | Ni | Zn | Pb | As | Se | Sr | Mo | Cd | Sb | Cu |
|--------|------|------|---------|------|-------|------|------|-------|------|-------|------|------|------|------|------|-------|------|------|
| Unit | min | L | pH unit | mV | μS/cm | μg/L | μg/L | μg/L | μg/L | μg/L | μg/L | μg/L | μg/L | μg/L | μg/L | μg/L | μg/L | μg/L |
| DL | | | | | | 0.1 | 10 | 0.005 | 0.3 | 0.5 | 0.01 | 0.03 | 0.2 | 0.04 | 0.1 | 0.01 | 0.01 | 0.2 |
| TOS-1 | 0 | 0.14 | 7.77 | 122 | 2420 | 80.9 | 830 | 1.85 | 3.8 | 2380 | 98.1 | 2.25 | 1.5 | 520 | 6.4 | 8.73 | 1.59 | 10.4 |
| TOS-2 | 30 | 0.65 | 7.92 | 126 | 1850 | 10.9 | 250 | 1.04 | 2 | 1720 | 52.9 | 0.84 | 1.3 | 380 | 5.8 | 7.22 | 1.05 | 5.9 |
| TOS-3 | 90 | 0.65 | 7.99 | 132 | 1030 | 4.1 | 130 | 0.61 | 1.3 | 1150 | 43.6 | 0.46 | 0.7 | 154 | 4.3 | 2.87 | 1.04 | 5.1 |
| TOS-4 | 180 | 1.96 | 7.76 | 130 | 660 | 3.3 | 80 | 0.52 | 1.1 | 799 | 43.7 | 0.28 | <0.2 | 84.2 | 5.2 | 2.24 | 1.01 | 5.6 |
| TOS-5 | 300 | 2.62 | 7.86 | 130 | 520 | 2.5 | 60 | 0.36 | 0.7 | 592 | 43 | 0.3 | 0.4 | 64.8 | 8.1 | 1.54 | 0.96 | 4.3 |
| TOS-6 | 360 | 1.31 | 7.9 | 131 | 490 | 2.5 | 60 | 0.37 | 0.7 | 535 | 43.6 | 0.28 | 0.7 | 60.2 | 9.0 | 1.41 | 1.02 | 3.9 |
| EM-1 | 0 | 0.14 | 6.66 | 143 | 470 | 521 | 40 | 106 | 51 | 42000 | 340 | 1.19 | 4.3 | 130 | <0.1 | 360 | 2.85 | 26.7 |
| EM-2 | 30 | 0.65 | 6.79 | 140 | 350 | 265 | 30 | 53.6 | 26.6 | 25300 | 410 | 0.81 | 2.4 | 90.7 | <0.1 | 196 | 2.26 | 16.6 |
| EM-3 | 90 | 0.65 | 7.2 | 146 | 310 | 154 | <10 | 27.4 | 13.8 | 14300 | 290 | 0.46 | 1.5 | 105 | <0.1 | 107 | 1.88 | 7.9 |
| EM-4 | 180 | 1.96 | 7.36 | 148 | 280 | 96.7 | <10 | 17.1 | 9.2 | 8580 | 195 | 0.42 | 1.7 | 114 | 0.4 | 66.8 | 1.9 | 9.5 |
| EM-5 | 300 | 2.62 | 7.48 | 148 | 270 | 68.5 | 10 | 12.4 | 6.8 | 5690 | 194 | 0.37 | 1.4 | 119 | 2.4 | 46.1 | 1.82 | 6.4 |
| EM-6 | 360 | 1.31 | 7.5 | 146 | 260 | 51.1 | 10 | 9.5 | 5.3 | 4520 | 171 | 0.35 | 1.6 | 121 | 4.6 | 35.2 | 1.78 | 4.6 |
| LMW | ---- | --- | --- | ---- | <100 | <0.1 | < 10 | 0.01 | <0.3 | 1.4 | 0.03 | 0.75 | 0.6 | 129 | 10.5 | <0.01 | 0.18 | <0.2 |
| MCL* | ---- | --- | ---- | ---- | ---- | ---- | ---- | ---- | 120 | 1200 | 150 | 60 | 40 | ---- | 200 | 20 | 100 | 600 |

LMW: low mineralized water used in the leaching tests. (*)MCL: maximum contaminated level of leachates (percolation test) of solid wastes, in order to deposit in landfills (inert solid wastes).

Table 5b.- Main anion contents of leachates.

| Analyte Symbol | time | F | Cl | NO ₂ (as N) | Br | NO ₃ (as N) | PO ₄ (as P) | SO ₄ | HCO ₃ (-) |
|-----------------|------|------|------|------------------------|-------|------------------------|------------------------|-----------------|----------------------|
| Unit Symbol | min | mg/L | mg/L | mg/L | mg/L | mg/L | mg/L | mg/L | mg/L |
| Detection Limit | --- | 0.01 | 0.03 | 0.01 | 0.03 | 0.01 | 0.02 | 0.03 | 1 |
| TOS-1 | 0 | 2.3 | 36.4 | 0.33 | <0.6 | 34.3 | <0.4 | 1790 | 72 |
| TOS-6 | 360 | 3.86 | 6.57 | <0.02 | <0.06 | 0.4 | <0.04 | 143 | 99 |
| EM-1 | 0 | 3.72 | 40.7 | <0.03 | <0.09 | 1.48 | <0.06 | 306 | 45 |
| EM-6 | 360 | 3.27 | 7 | <0.01 | <0.03 | 0.43 | <0.02 | 27 | 99 |
| LMW | --- | 1.0 | 6.85 | <0.01 | <0.03 | 0.66 | <0.02 | 10.9 | 99 |
| MCL* | --- | 40 | 8500 | --- | --- | --- | --- | 7000 | --- |

Table 6.- Calculated saturation index for water samples and leachates. Saturation indices calculated using PHREEQC and database MINTEQ. *: Coral adit. EM-1, TOS-1: leachates.

| Mineral phase | OS-6(S) | OS-7(S) | OS-8(S)* | OS-9(S) | OS-10(S) | OS-11(S)* | EM-1 | TOS-1 |
|---------------------------------------|---------|---------|----------|---------|----------|-----------|-------|-------|
| Iron oxyhydroxides | | | | | | | | |
| Fe(OH) ₃ | 0.30 | 1.00 | 1.05 | 1.18 | 1.10 | 0.76 | -2.08 | 1.97 |
| Goethite | 4.44 | 5.13 | 5.18 | 5.32 | 5.23 | 4.90 | 2.08 | 6.13 |
| Sulphate minerals | | | | | | | | |
| Jarosite | -4.72 | -3.2 | -0.79 | -1.7 | -3.18 | 0.34 | -6.45 | 3.97 |
| Jarosite-Na | -7.15 | -5.68 | -3.62 | -4.24 | -5.70 | -2.28 | -9.17 | 0.58 |
| Gypsum | -2.72 | -2.47 | -0.92 | -1.86 | -2.54 | -0.65 | -1.00 | 0.24 |
| Lead minerals | | | | | | | | |
| Anglesite | -5.52 | -6.28 | -5.32 | -5.55 | -5.80 | -3.79 | -1.43 | -2.40 |
| Cerrusite | -2.12 | -2.52 | -1.96 | -2.15 | -2.46 | -1.12 | -0.23 | -0.44 |
| Zinc minerals | | | | | | | | |
| Smithsonite | -1.94 | -2.31 | -0.17 | -0.81 | -2.60 | -0.54 | -0.50 | -0.81 |
| ZnCO ₃ ·H ₂ O | -1.61 | -1.97 | 0.17 | -0.48 | -2.26 | -0.20 | -0.17 | -0.48 |
| Hydrocincite | 29.4 | 28.4 | 37.9 | 35.6 | 28.5 | 34.3 | 35.7 | 37.1 |
| Carbonate & other minerals | | | | | | | | |
| Calcite | -2.72 | -0.52 | 0.65 | -0.27 | -1.00 | 0.22 | -1.59 | 0.40 |
| Dolomite | -1.12 | -1.52 | 0.67 | -1.08 | -2.40 | -0.18 | -3.79 | 0.23 |
| Siderite | -2.27 | -2.29 | -1.83 | -1.88 | -2.53 | -0.52 | -2.87 | -0.54 |
| Gibbsite | 0.05 | 0.34 | -0.28 | 0.21 | 0.29 | 0.82 | -1.17 | 1.46 |
| SiO ₂ (am) | -1.19 | -1.34 | -1.28 | -1.23 | -1.23 | -1.22 | -1.4 | -1.74 |
| Kaolinite | 4.16 | 4.45 | 3.31 | 4.4 | 4.55 | 5.63 | 1.3 | 5.85 |

FIG. CAPTIONS

Fig. 1.- Situation map of the study area. Synthetic geologic map and soil, mine wastes, and waters sampling points.

Fig. 2.- Piper diagram of selected samples (superficial water, mine water, and leachate EM-6).

Fig. 3.- Evolution of Zn with time for leaching experiments.

Fig. 4.- Evolution of Mn with time for leaching experiments.

Fig. 5.- (Ca+Mg) vs. (HCO₃+SO₄) scatter diagram of water samples.

Fig. 6.- Evaluation of Mn, Fe and Ni mobilization from Coral adit to Osor creek at summer, winter and autumn.

Fig. 7.- Evaluation of Zn, Cd, Pb and SO₄⁻² mobilization from Coral adit to Osor creek at summer, winter and autumn.